Inorganic Chemistry Communications 51 (2015) 66–70

Contents lists available at ScienceDirect

Inorganic Chemistry Communications

journal homepage: www.elsevier.com/locate/inoche

Synthesis and studies of a molecular molybdenum–Schiff base electrocatalyst for generating hydrogen from organic acid or water

Ting Fang, Hai-Xia Lu, Jia-Xing Zhao, Shu-Zhong Zhan *

College of Chemistry and Chemical Engineering, South China University of Technology, Guangzhou 510640, China

ARTICLE INFO

Article history:
Received 2 August 2014
Received in revised form 25 October 2014
Accepted 10 November 2014
Available online 12 November 2014

Keywords:
Molybdenum(VI) complex
Molecular structure
Molecular electrocatalyst
Hydrogen evolution

ABSTRACT

The reaction of N,N-dimethylethylenediamino-N,N-bis(2,4-dimethylphenol) (H_2L) (H_2L) and $MoCl_5$ gives a Mo(VI) complex $[MoL(O)_2]$ **1**, which has been determined by X-ray crystallography. Electrochemical studies show that complex **1** can catalyze hydrogen evolution from acetic acid, trifluoroacetic acid and water with a turnover frequency (TOF) of 25.72 (acetic acid), 101.15 (trifluoroacetic acid) and 676 (buffer, pH 7.0) moles of hydrogen per mole of catalyst per hour, respectively.

Hydrogen, when derived from carbon-neutral processes, is an attractive clean fuel candidate for renewable energy storage and transport [1–3]. In nature, hydrogenase enzymes [4–6] can efficiently catalyze both the production and the oxidation of hydrogen using earth-abundant metals (such as nickel and iron). However, enzymes are difficult to obtain in sufficient amounts to adapt for commercial applications and their stability is often limited outside of their native environment.

These considerations have led to the development of molecular catalysts employing more abundant metals, and several complexes that contain nickel, iron, copper and cobalt which have been developed as electrocatalysts for the production of hydrogen [7–21].

A recent report from Chang and co-workers described a highly active molecular molybdenum electrocatalyst, $[(Py_5Me_2)MoO]^{2+}$ (Py_5Me_2 = 2,6-bis(1,1-bis(2-pyridyl)ethyl)pyridine, a neutral pentadentate ligand) that reduces water to H_2 at neutral pH in aqueous buffer [22]. It has been shown that the donor type and electronic properties of the ligands play vital roles in determining the structure and reactivity of the corresponding metal complexes. Identification of the factors that control the oxidation/reduction site in these complexes, determining of their redox potentials and characterization of their electronic structures are critical for the design of more effective molecular electrocatalysts for H_2 production. With this in mind, we chose tetradentate ligands, such as H_2L, a potential deprotonated ligand to react with $MoCl_5$ to construct the corresponding Mo complex, and explore its electrocatalytic properties. In this paper, we present the synthesis, structure and properties of a new molybdenum(VI) complex $[MoL(O_2)]$ **1**, as well as its catalytic function for hydrogen evolution from acetic acid or water thereof.

The reaction of ligand, H_2L ([23], Figs. S1–S2) and $MoCl_5$ affords yellow crystals of complex **1** (Scheme 1, [24]), which is air stable in the solid state or liquid state, solvable in DMF, CH_2Cl_2, and CH_3CN. The IR spectrum of complex **1** displays two strong $\nu_{Mo=O}$ bands at 960 and 913 cm^{-1} (Fig. S3), characteristic for symmetric and asymmetric vibrational modes, respectively, of the *cis*-$[MoO_2]^{2+}$ fragment [25,26].

Crystallographic data for complex **1** are given in Table S1 and selected bond lengths are listed in Table S2. As shown in Fig. 1, X-ray structure of complex **1** reveals a six-coordinate Mo atom in a distorted octahedral surrounding, with a *fac* coordination of the ligand. The molybdenum oxo groups show the expected mutual *cis* configuration. The Mo═O bond lengths (Mo–O3, 1.7010(15) Å; Mo–O4, 1.6999(16) Å) are in the expected range of *cis*-dioxo Mo^{VI} complexes [27,28].

As shown in Fig. 2, cyclic voltammogram of complex **1** exhibits two reversible couples at −1.17 V and −1.32 V versus Ag/$AgNO_3$, which can be assigned to $Mo^{VI/V}$ and $Mo^{V/IV}$, respectively. The current responses of the redox events at −1.17 V and −1.32 V show linear dependence on the square root of the scan rate (Fig. S4), which is an indicative of a diffusion-controlled process, with the electrochemically active species freely diffusing in the solution.

To determine possible electrocatalytic activity of this complex, cyclic voltammograms of complex **1** were recorded in the presence of acetic acid. Fig. 3-a shows a systematic increase in i_{cat} observed near −1.32 V with increasing acetic acid concentration from 0.0 to 45 mM. The second redox wave depicted in Fig. 3-a is dependent of acid concentration, indicating that this one electron-transfer step is devoted to proton reduction.

---

* Corresponding author.
E-mail address: shzhzhan@scut.edu.cn (S.-Z. Zhan).

http://dx.doi.org/10.1016/j.inoche.2014.11.009

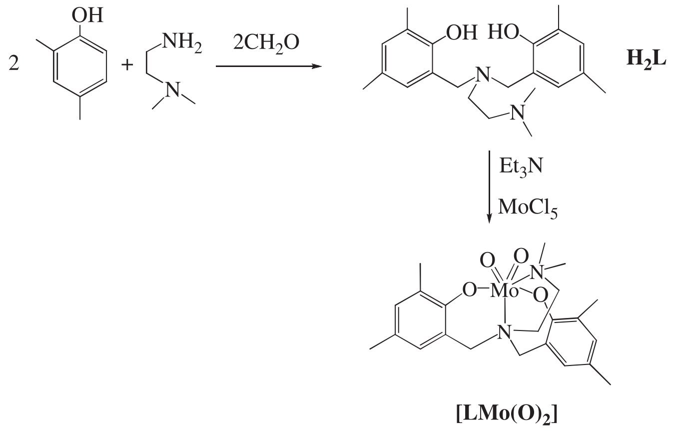

Scheme 1. Schematic representation of the synthesis of complex $[LMo(O)_2]$.

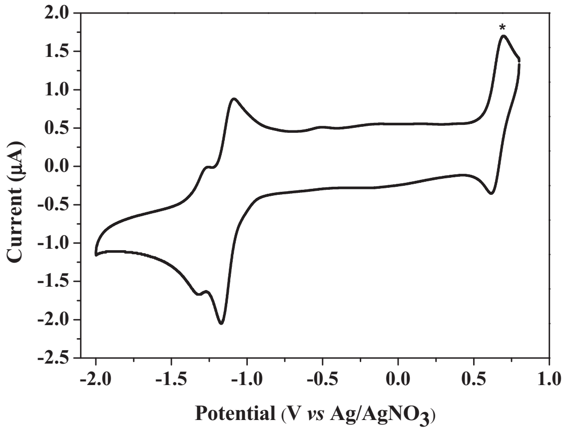

Fig. 2. Cyclic voltammogram of complex **1** in 0.1 M of $[n\text{-}Bu_4N]ClO_4$ DMF solution at a glassy carbon electrode and a scan rate of 100 mV/s. Ferrocene internal standard (*).

The onset of this catalytic current is clearly influenced by the acid concentration, the applied potential declines with increasing acid concentration. Cyclic voltammogram of background in the absence of **1** exhibits no catalytic current at the potential of the couple of $Mo^{V/IV}$ (Fig. S5), suggesting that proton reduction to H_2 occurs with **1** and a Mo(IV) intermediate is responsible for the reductive proton to generate H_2 [22], with catalytic onset shift to more positive potential (from −0.93 to −0.67 V). On the basis of literature precedent [22,29] and above analyses, we postulate the catalytic cycle depicted in Scheme 2 for the generation of hydrogen from acid mediated by **1**. Two-electron reduction of $[Mo^{VI}L(O)_2]$ gives $[Mo^{IV}L(O)_2]^{2-}$. Addition of proton produces the reactive intermediate $[Mo^{IV}L(OH)_2]$ and then affords H_2 and gives rise to a cycle in which $[Mo^{IV}L(OH)_2]$ precedes the formation of $[Mo^{VI}L(O)_2]$ **1**.

We also used trifluoroacetic acid as proton source to test the catalytic function of complex **1**. Fig. 3-b also exhibits a systematic increase in i_{cat} observed near −1.32 V with increasing trifluoroacetic acid concentration from 0.67 to 20.0 mM. This rise in current also can be attributed to the catalytic generation of H_2 from trifluoroacetic acetic acid with catalytic onset shift to more positive potentials (from −1.10 to −0.35 V). Further evidence for the electro-catalytic activity was obtained by bulk electrolysis of a DMF solution of complex **1** (16.3 μM) with acetic acid (2.70 mM) or trifluoroacetic acid (1.20 mM) at variable applied potential. Fig. 4 shows the total charge of bulk electrolysis of complex **1** in the presence of acid, the charge significantly increased when the applied potential was set to more negative. According to Eq. (1) [22], we calculated TOF for the catalyst reaching a maximum of 25.72 (acetic acid) and 101.15 (trifluoroacetic acid) moles of hydrogen per mole of catalyst per hour (Eq. (2) in Supplementary material 4 and Fig. S6). The value (25.72) is lower than that of $[LMo^{VI}(O)_2]$ (L = 2-pyridylamino-N,N-bis(2-methylene-4,6-difluorophenol) ion) (50.6 mol of hydrogen per mole of catalyst per hour), a similar type of complex [29]. This is consistent with an evident increase in the catalytic activity when electron-withdrawing groups are present at the phenol para-position of the ligand [30].

$$\mathrm{TOF} = \Delta C / (\mathrm{F} * n_1 * n_2 * t) \tag{1}$$

We also tried to explore the catalytic hydrogen evolution in aqueous media, a much more attractive medium for the sustainable generation of hydrogen. CVs were conducted in 0.25 M phosphate buffers at different pH values. As shown in Fig. S7-(a), in the absence of complex **1**, a catalytic current was not apparent until a potential of −1.50 V versus

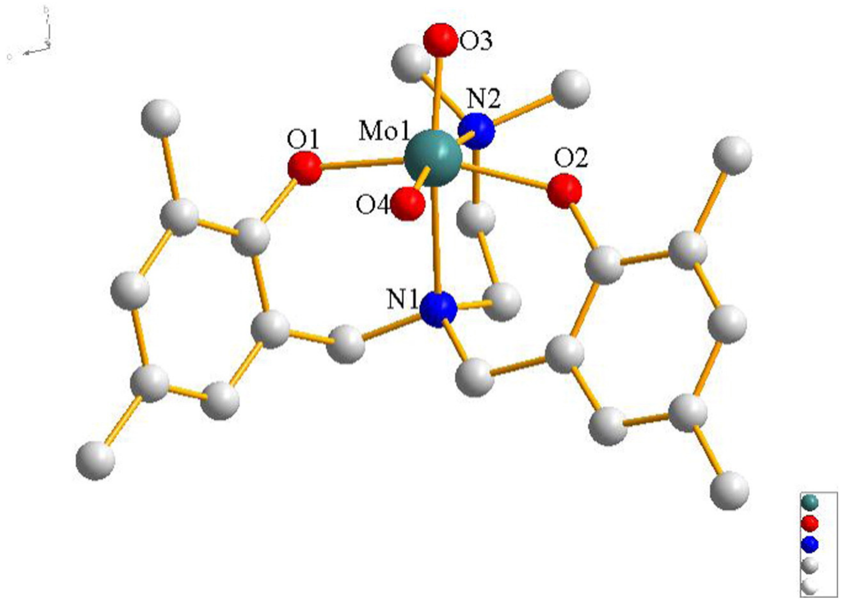

Fig. 1. Molecular structure of **1**.

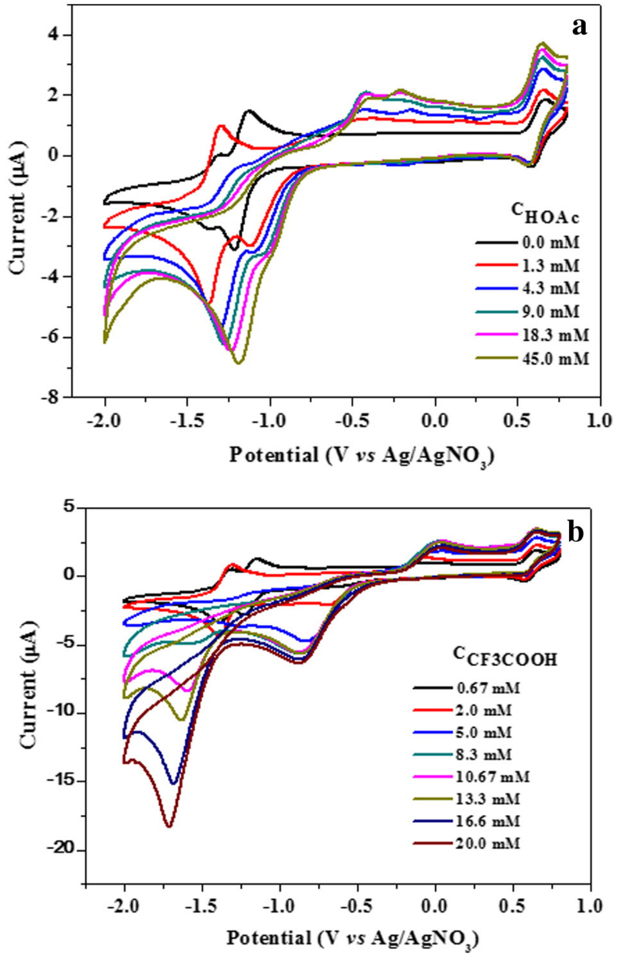

Fig. 3. Cyclic voltammograms of a 1.7 mM solution of complex **1**, with varying concentrations of acetic acid (a) and trifluoroacetic acid (b) in DMF. Conditions: r.t., 0.1 M [n-Bu_4N] ClO_4 as supporting electrolyte, scan rate: 100 mV/s, GC working electrode (1 mm diameter), Pt counter electrode, Ag/$AgNO_3$ reference electrode, Fc internal standard.

Ag/AgCl was attained. With addition of complex **1**, the onset of catalytic current was observed at about − 1.20 V versus Ag/AgCl, and the current strength increased significantly with increasing concentrations of complex **1** from 0.00 to 0.04 mM. The potential moved positive about 600 mV compared to that in the absence of complex **1** (from 1.50 to 0.90 V). Furthermore, it is found that the catalytic current maximum of **1** was also dependent on pH values of buffers (Fig. S8), indicating that this catalyst is functioning in a diffusion-controlled regime.

Catalytic hydrogen production can also be achieved with complex **1** in buffer, Fig. 5 shows the total charge of bulk electrolysis of the solution containing complex **1** at pH 7.0. When applied potential is − 1.40 V versus Ag/AgCl at pH 7.0, the maximum charge was only 56.5 mC during 2 min of electrolysis in the absence of complex **1** (Fig. S9). Under the same conditions, the charge reached 940 mC with addition of complex **1** (0.82 μM), which was confirmed to be H_2 by GC analysis. The evolved H_2 was analyzed by gas chromatography, Fig. S10, which gave ~ 11.4 mL of H_2 over an electrolysis period of 1 h. TOF for complex **1** is 676 (pH 7.0) Eq. (3) in Supplementary material 4) moles of hydrogen per mole of catalyst per hour (Fig. S11). The value (676 mol of hydrogen per mole of catalyst per hour) is lower than that of $[(Py_5Me_2)MoIVO]^{2+}$ [22], indicating that the molybdenum(IV) electrocatalyst is more active than the molybdenum(VI) species.

We have successfully prepared a new molybdenum(VI) complex **1**, that can catalyze hydrogen evolution not only from acetic acid or trifluoroacetic acid but also from water. Ongoing efforts are focused on modifying Schiff base ligands and generating the related water-soluble complexes to further facilitate new functional studies.

Acknowledgments

This work was supported by the National Science Foundation of China (No. 20971045, 21271073), and the Student Research Program (SRP) of South China University of Technology (No. B15-B7050170).

Appendix A. Supplementary material

CCDC 1005596 contains the Supplementary crystallographic data for this paper. This data can be obtained free of charge via http://www.ccdc.cam.ac.uk/conts/retrieving.html, or from the Cambridge Crystallographic Data Centre, 12 Union Road, Cambridge CB2 1EZ, UK; fax: (+44) 1223-336-033; or e-mail: deposit@ccdc.cam.ac.uk. Supplementary data associated with this article can be found, in the online version, at http://dx.doi.org/10.1016/j.inoche.2014.11.009.

References

[1] J.A. Turner, Sustainable hydrogen production, Science 305 (2004) 972–974.
[2] J.R. McKone, S.C. Marinescu, B.S. Brunschwig, J.R. Winkler, H.B. Gray, Earth-abundant hydrogen evolution electrocatalysts, Chem. Sci. 5 (2014) 865–878.
[3] K.A. Vincent, A. Parkin, F.A. Armstrong, Investigating and exploiting the electrocatalytic properties of hydrogenases, Chem. Rev. 107 (2007) 4366–4413.
[4] J.C. Fontecilla-Camps, A. Volbeda, C. Cavazza, Y. Nicolet, Structure/function relationships of [NiFe]- and [FeFe]-hydrogenases, Chem. Rev. 107 (2007) 4273–4303.
[5] P.M. Vignais, B. Billoud, Occurrence, classification, and biological function of hydrogenases: an overview, Chem. Rev. 107 (2007) 4206–4272.
[6] C.J. Pickett, C. Tard, Structural and functional analogues of the active sites of the [Fe]-, [NiFe]-, and [FeFe]-hydrogenases, Chem. Rev. 109 (2009) 2245–2274.
[7] M.Y. Darensbourg, W. Wegand, Sulfoxygenation of active site models of [NiFe] and [FeFe] hydrogenases — a commentary on possible chemical models of hydrogenase enzyme oxygen sensitivity, Eur. J. Inorg. Chem. 2011 (2011) 994–1004.
[8] M.Y. Darensbourg, E.J. Lyon, J.J. Smee, The bio-organometallic chemistry of active site iron in hydrogenases, Coord. Chem. Rev. 206 (2000) 533–561.
[9] A.C. Marr, D.J.E. Spencer, M. Schroder, Structural mimics for the active site of [NiFe] hydrogenase, Coord. Chem. Rev. 219 (2001) 1055–1074.
[10] A.D. Nguyen, M.D. Rail, M. Shanmugam, J.C. Fettinger, L.A. Berben, Electrocatalytic hydrogen evolution from water by a series of iron carbonyl clusters, Inorg. Chem. 52 (2013) 12847–12854.
[11] F. Quentel, G. Passard, F. Gloaguen, Electrochemical hydrogen production in aqueous micellar solution by a diiron benzenedithiolate complex relevant to [FeFe] hydrogenases, Energy Environ. Sci. 5 (2012) 7757–7761.
[12] M.Y. Darensbourg, E.J. Lyon, X. Zhao, I.P. Georgakaki, The organometallic active site of [Fe] hydrogenase: models and entatic states, Proc. Natl. Acad. Sci. U. S. A. 100 (2003) 3683–3688.
[13] D.J. Evans, C.J. Pickett, Chemistry and the hydrogenases, Chem. Soc. Rev. 32 (2003) 268–275.
[14] S. Canaguier, V. Fourmond, C.U. Perotto, J. Fize, J. Pecaut, M. Fontecave, M.J. Fielde, V. Artero, Catalytic hydrogen production by a Ni–Ru mimic of NiFe hydrogenases involves a proton-coupled electron transfer step, Chem. Commun. 49 (2013) 5004–5006.
[15] M.E. Carroll, B.E. Barton, T.B. Rauchfuss, P.J. Carroll, Synthetic models for the active site of the [FeFe]-hydrogenase: catalytic proton reduction and the structure of the doubly protonated intermediate, J. Am. Chem. Soc. 134 (2012) 18843–18852.
[16] N. Wang, M. Wang, Y. Wang, D. Zheng, H. Han, M.S.G. Ahlquist, L. Sun, Catalytic activation of H_2 under mild conditions by an [FeFe]-hydrogenase model via an active μ-hydride species, J. Am. Chem. Soc. 135 (2013) 13688–13691.
[17] M.A. Gross, A. Reynal, J.R. Durrant, E. Reisner, Versatile photocatalytic systems for H_2 generation in water based on an efficient DuBois-type nickel catalyst, J. Am. Chem. Soc. 136 (2014) 356–366.
[18] W.M. Singh, T. Baine, S. Kudo, S. Tian, X.A.N. Ma, H. Zhou, Electrocatalytic and photocatalytic hydrogen production in aqueous solution by a molecular cobalt complex, Angew. Chem. Int. Ed. 51 (2012) 5941–5944.
[19] J.P. Cao, T. Fang, L.Z. Fu, L.L. Zhou, S.Z. Zhan, A nickel molecular electro-catalyst for generating hydrogen from acetic acid or water, Int. J. Hydrogen Energy 39 (2014) 10980–10986.
[20] J.P. Cao, T. Fang, Z.Q. Wang, Y.W. Ren, S.Z. Zhan, A dinuclear triazenido–copper complex: a new molecular electro-catalyst for generating hydrogen from acetic acid or water, J. Mol. Catal. A Chem. 391 (2014) 191–197.
[21] V.S. Thoi, H.I. Karunadasa, Y. Surendranath, J.R. Long, C.J. Chang, Electrochemical generation of hydrogen from acetic acid using a molecular molybdenum–oxo catalyst, Energy Environ. Sci. 5 (2012) 7762–7770.
[22] H.I. Karunadasa, C.J. Chang, J.R. Long, A molecular molybdenum–oxo catalyst for generating hydrogen from water, Nature 464 (2010) 1329–1333.
[23] Synthesis of N,N-dimethylethylenediamino-N,N-bis(2,4-dimethylphenol) (H_2L).A solution of 2,4-dimethylphenol (2.44 g, 20 mmol), N,N-dimethylethylenediamine (0.88 g, 10 mmol), and 37% aqueous formaldehyde (1.62 g, 20 mmol) in water (50 mL) was stirred and refluxed for 8 h. Upon cooling, a large quantity of beige solid formed. The solvents were decanted, and the remaining solid residue was washed with cold ethanol to give a pure, white powder (2.415 g, 67.8% yield). Crystalline product was obtained by slow cooling of a hot diethyl ether solution.

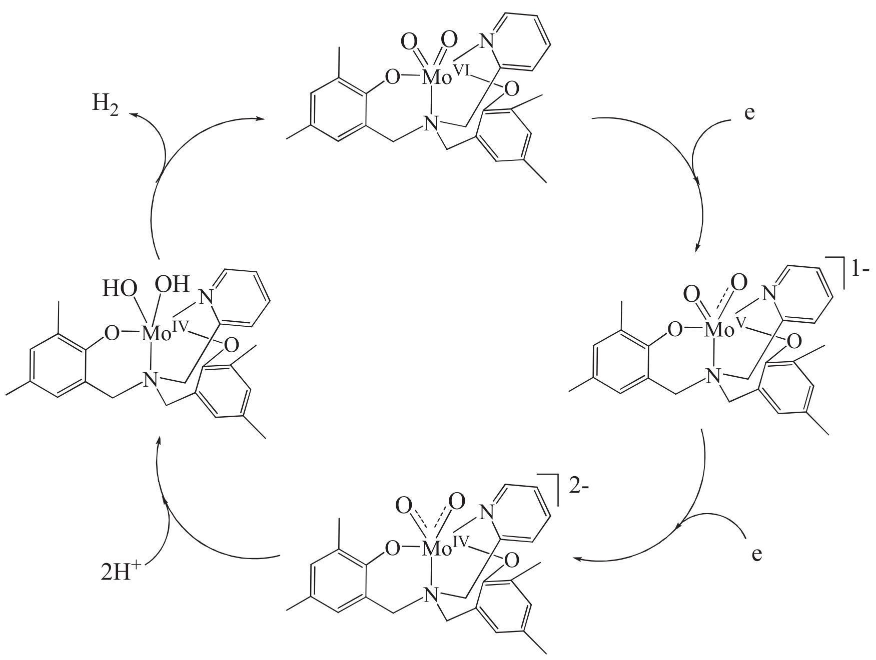

Scheme 2. The possible catalytic mechanism by $[MoL(O)_2]$ **1**.

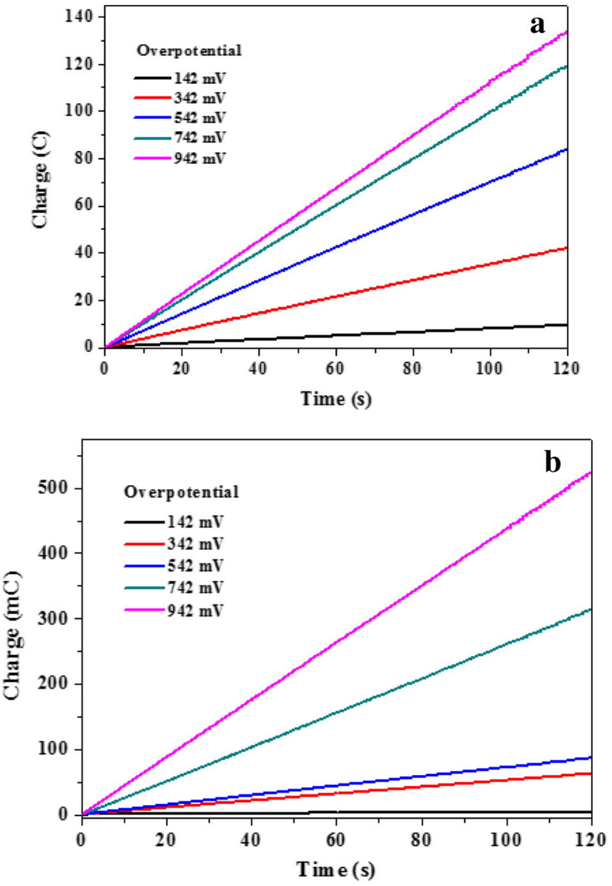

Fig. 4. Charge buildup versus time from electrolysis of a 16.3 μM complex **1** in 2.70 mM acetic acid (a) and 1.20 mM trifluoroacetic acid (b) under various overpotentials. All data have been deducted blank.

Anal. calcd for $C_{22}H_{32}N_2O_2$: C, 74.16; H, 8.99; N, 7.86%. Found C, 74.33; H, 8.88; N, 7.81%. ^{1}H NMR (400 MHz, $CDCl_3$) δ 6.84 (s, 2H), 6.66 (s, 2H), 3.57 (s, 4H), 2.55 (s, 4H), 2.30 (s,6H), 2.19 (s, 12H) (Figure S1). ^{13}C NMR (100 MHz, $CDCl_3$) δ 152.723, 131.285, 128.424, 127.481, 125.507, 121.674, 77.163, 56.509, 56.171, 49.191, 45.093, 20.496, 16.273 (Figure S2).

[24] Synthesis of complex **1**.To a solution, containing H_2L (0.28 g, 0.5 mmol) and pyridine (0.04 g, 0.5 mmol) in acetonitrile/methanol (10 mL, 1:1), $MoCl_5$ (0.14 g, 0.5 mmol) was added and the mixture was stirred for 5 min. Single crystals were obtained from the filtrate which was allowed to stand at room temperature for several days, collected by filtration, and dried in *vacuo* (0.12 g, 48%). The elemental analysis results (found C, 54.67; H, 6.01; N, 5.78. $C_{32}H_{42}N_2O_4Mo$ requires C, 54.84; H, 6.02; N, 5.82) were in agreement with the formula of the sample used for X-ray analysis.

[25] B.E. Schultz, S.F. Gheller, M.C. Muetterties, M.J. Scott, R.H. Holm, Molybdenum-mediated oxygen-atom transfer: an improved analog reaction system of the molybdenum oxotransferases, J. Am. Chem. Soc. 115 (1993) 2714–2722.

[26] L.M. Thomson, M.B. Hall, A theoretical study of the primary oxo transfer reaction of a dioxo molybdenum(VI) compound with imine thiolate chelating ligands: a molybdenum oxotransferase analogue, J. Am. Chem. Soc. 123 (2001) 3995–4002.

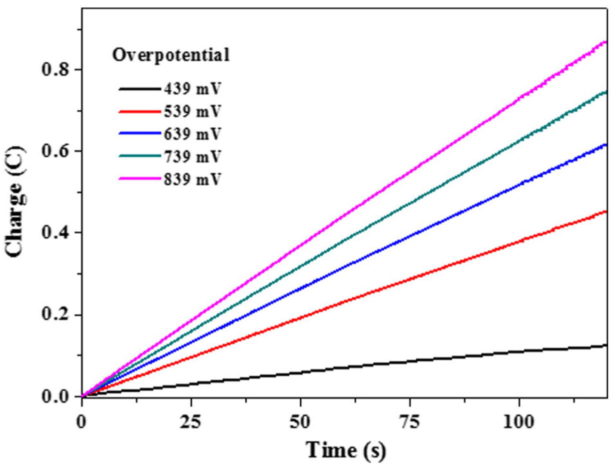

Fig. 5. Charge buildup of complex **1** (0.82 μM) versus overpotentials (mV vs SHE) at pH 7.0. All data have been deducted blank.

[27] G. Lyashenko, R. Herbst-Irmer, V. Jancik, A. Pal, N.C. Mosch-Zanetti, Molybdenum oxo and imido complexes of β-diketiminate ligands: synthesis and structural aspects, Inorg. Chem. 47 (2008) 113–120.

[28] B.L. Tran, C.J. Carrano, Oxo–molybdenum(VI, V, IV) complexes of the facially coordinating tris(mercaptoimidazolyl)borate ligand: synthesis, characterization, and oxygen atom transfer reactivity, Inorg. Chem. 46 (2007) 5429–5438.

[29] J.-P. Cao, L.-L. Zhou, L.-Z. Fu, S.-Z. Zhan, A molecular molybdenum electrocatalyst for generating hydrogen from acetic acid or water, J. Power Sources 272 (2014) 169–175.

[30] Z. Codolà, I. Garcia-Bosch, F. Acuña-Parés, I. Prat, J.M. Luis, M. Costas, J. Lloret-Fillol, Electronic effects on single-site iron catalysts for water oxidation, Chem. Eur. J. 19 (2013) 8042–8047.